Optik 127 (2016) 4447–4453

Contents lists available at ScienceDirect

Optik

journal homepage: www.elsevier.de/ijleo

Nonclassical effects in the second harmonic generation

Horacio Grinberg*

Department of Physics, Facultad de Ciencias Exactas y Naturales, University of Buenos Aires, Pabellón 1, Ciudad Universitaria, 1428 Buenos Aires, Argentina

ARTICLE INFO

Article history:
Received 14 December 2015
Accepted 18 January 2016

Keywords:
Second harmonic
Variance squeezing
Quantum entanglement
Coherent state
Information entropy

ABSTRACT

The higher-order nonclassical squeezing and quantum entanglement effects emerging from the second harmonic generation of the associated two-mode and two-photon Hamiltonian are investigated in the dispersive limit. The squeezed states of the field, including the normal and amplitude squared (higher-order) squeezing factors are generated in two ways, i.e., from the bosonic operators via amplitude powered quadrature variables, and through the $SU(2)$ characterization of a passive and lossless device with two input and two output ports, which then allows one to visualize the operations of beam splitters and phase shifters as rotations of angular momentum operators in 3-space. Two criteria for intermodal higher-order quantum entanglement and different coherent states for the two modes in the initial state are used to compute these nonclassical effects. The unitary time evolution of the linear entropy, computed from the partial trace of the density matrix over the secondary mode, is also used as a criterion of quantum entanglement. These approaches show, in fact, that the present model exhibits a considerable amount of this nonclassical effect. The unitary time evolution of the linear entropy shows that the present nonlinear optical model does not preserve the modulus of the Bloch vector.

1. Introduction

Second harmonic generation (SHG) is a nonlinear optical process, in which photons with the same frequency interacting with a nonlinear material are effectively "combined" to generate new photons with twice the energy, and therefore twice the frequency and half the wavelength of the initial photons. In biological and medical science, the effect of SHG is used for high-resolution optical microscopy. Because of the non-zero second harmonic coefficient, only non-centrosymmetric structures are capable of emitting SHG light. One such structure is collagen, which is found in most load-bearing tissues. SHG microscopy has been used for extensive studies of the cornea [1] and lamina cribrosa sclerae [2], both of which consist primarily of collagen. SHG is also used by the laser industry to make green 532 nm lasers from a 1064 nm source and for measuring ultra short pulse width by means of intensity auto-correlation. Generating the second harmonic, often called frequency doubling, is also a process in radio communication; it was developed in the 20th century, and has been used with frequencies in the megahertz range.

Generally speaking, these *two-photon states* can be useful for solving various fundamental physical and technological problems. For example, one can use the two-photon states in order to improve optical communications by reducing the quantum fluctuations in one (signal) quadrature component of the field at the expense of the amplified fluctuations in another (unobservable) component. These interesting properties and applications in various fields of applied and basic theoretical research of the SHG, motivated us to explore the so far uninvestigated potential existence of nonclassical squeezing and intermodal higher-order quantum entanglement effects in the associated electromagnetic field. In this context it is worth noting that several new applications of these nonclassical states have been reported in recent past [3–7]. As a consequence of these recently reported applications, generation of nonclassical states in various quantum systems emerged as one of the most important areas of interest in quantum information theory and quantum optics [8,9]. Several systems are already investigated and have been shown to produce entanglement and other nonclassical states [10,11].

A state having negative or highly singular (more singular than δ function) Glauber–Sudarshan P function is referred to as a nonclassical state as it cannot be expressed as a classical mixture of coherent states [3]. P function provides us an essential as well as sufficient criterion for detection of nonclassicality. However, P function is not directly experimentally measurable. Consequently, several operational criteria for nonclassicality have

* Correspondence to: IFIBA, Consejo Nacional de Investigaciones Científicas y Técnicas, Argentina. Tel.: +54 11 4576 3353; fax: +54 11 4576 3357.
E-mail address: grinberg@df.uba.ar

http://dx.doi.org/10.1016/j.ijleo.2016.01.152
0030-4026/

been proposed in the past. A large number of these criteria are expressed as inequalities involving expectation values of functions of annihilation and creation operators. As mentioned above we are interested in the higher-order nonclassical properties of radiation fields. In quantum optics and quantum information higher-order nonclassical properties of bosons (e.g., higher-order Hong-Mandel squeezing, higher-order antibunching, higher-order sub-Poissonian statistics, higher-order entanglement, etc.) are often studied [12]. Until recently, past studies on higher-order nonclassicalities were predominantly restricted to theoretical investigations. However, a bunch of exciting experimental demonstrations of higher-order nonclassicalities have been recently reported [13–15].

Higher-order squeezing is usually studied using two different approaches. In the first approach introduced by Hillery [16] reduction of variance of an amplitude powered quadrature variable for a quantum state with respect to its coherent state counterpart reflects nonclassicality. In contrast, in the second type of higher-order squeezing introduced by Hong and Mandel [17,18], higher-order squeezing is reflected through the reduction of higher-order moments of usual quadrature operators with respect to their coherent state counterparts.

The present contribution aims to study higher-order nonclassical properties emerging from the SHG Hamiltonian with specific attention to higher-order squeezing and higher-order quantum entanglement.

The remaining part of the paper is organized as follows. Section 2 introduces the theoretical background associated with the SHG Hamiltonian together with the two approaches of squeezing based on the variances of the quadrature modes. We also introduce a scattering matrix, proper of the $SU(2)$ group, which will in general transform the angular momentum operators among themselves. Since $SU(2)$ is equivalent to the rotation group in three dimensions, introduction of the Schwinger representation of the angular momentum operators through an homomorphism with the unitary group, will allow one to visualize the operations of beam splitter and phase shifters as rotations in 3-space. This section ends with the description of the conditions for the intermodal higher-order quantum entanglement. In Section 3 we use the criteria described in the previous section to numerically illustrate the nonclassical character of the radiation field of this nonlinear optical process using different initial coherent states. This is a novel feature of the present approach, since coherent states can be considered as squeezed states. It will be shown that the variances of different canonically conjugated variables can even assume (small) values which are less than the ground state variances. It will be also shown that there exists the possibility of a weak intermodal higher-order quantum entanglement of this specific two-mode optical process. This is reflected, in particular, in the unitary evolution of the linear entropy which shows that the present nonlinear optical process does not preserve the modulus of the Bloch vector. The paper ends up with conclusions in Section 4.

2. Theoretical background

2.1. Second harmonic generation Hamiltonian and initial conditions

With the widespread use of large-amplitude beams from powerful lasers, it is necessary to assume that the relationship between the polarization and the electric field is nonlinear. In fact, the second-order term of the expansion of the polarization in powers of the electric field shows that the resultant second-order nonlinear response generates an oscillating polarization at the sum and difference frequencies of the input fields. If the two frequencies are equal, the sum frequency is at twice the input frequency, and the effect is called frequency doubling or second harmonic generation. This nonlinear process is governed by the Hamiltonian

$$\mathcal{H} = \mathcal{H}_0 + \mathcal{H}_{\rm int} = \omega_a a^\dagger a + \omega_b b^\dagger b + g(a^2 b^\dagger + a^{\dagger 2} b), \tag{1}$$

where $a(a^\dagger)$ and $b(b^\dagger)$ are the annihilation (creation) operators of the fundamental mode of frequency ω_a and of the second hermonic mode of frequency ω_b, respectively, satisfying standard commutation relations for the Lie algebra of $SU(2)$. When perfect matching conditions are satisfied, we have the relation $\omega_a = 2\omega_b$. The constant g describes phenomenologically the coupling between the modes. It can always be chosen as real.

The nonlinear Hamiltonian (1) can be diagonalized through the method of small rotations pioneered by Klimov et al. [19,20] and we briefly describe it. After noting that it admits the constant of motion [19]

$$\mathcal{R} = a^\dagger a + 2b^\dagger b, \tag{2}$$

then the Hamiltonian can be rewritten in the following form

$$\begin{aligned} \mathcal{H}_0 &= \frac{\omega_a + \omega_b}{3}\mathcal{R} \\ \mathcal{H}_{\rm int} &= \frac{\Delta}{3}(b^\dagger b - a^\dagger a) + g(a^2 b^\dagger + a^{\dagger 2} b), \end{aligned} \tag{3}$$

where $\Delta = \omega_b - 2\omega_a$ is the detuning.

Since $\mathcal{H}_0$ determines the total energy stored in both modes, which is conserved, $[\mathcal{H}_0, \mathcal{H}_{\rm int}] = 0$, we can factor out $\exp(-i\mathcal{H}_0 t)$ from the evolution operator and drop it altogether.

In the present work we are interested in the dispersive limit of this model, when

$$|\Delta| \gg g(\bar{n}_1 + 1)(\bar{n}_2 + 1), \tag{4}$$

where $\bar{n}_1$ and $\bar{n}_2$ denote the average photon numbers in the first and second harmonic modes a and b, respectively. Then, using the Lie transformation method [19–21], and applying a unitary transformation to the interaction Hamiltonian (1), an effective Hamiltonian is obtained as

$$\mathcal{H}_{eff} = \mathcal{T}\mathcal{H}_{\rm int}\mathcal{T}^\dagger, \tag{5}$$

where

$$\mathcal{T} = \exp[\lambda(a^2 b^\dagger - a^{\dagger 2} b)], \tag{6}$$

with $\lambda = g/\Delta \ll 1$. By expanding Eq. (5) in a power series and keeping terms up to the order $(g/\Delta)^2$, yields

$$\mathcal{H}_{eff} = \frac{\Delta}{3}(b^\dagger b - a^\dagger a) + \frac{g^2}{\Delta}[4b^\dagger b a^\dagger a - (a^\dagger a)^2]. \tag{7}$$

The effective Hamiltonian Eq. (7) describes the dispersive evolution of the fields, but the essential point is that it is diagonal, which implies that there is no population transfer between the modes (as expected in the far resonant limit). The first term in Eq. (7) does not affect the dynamics and just leads to rapid oscillations of the wave function. The dynamics of the present model is not stationary and depends on the initial conditions of the model. Thus, it is assumed that, initially, the field modes are in generalized Glauber boson coherent states $|z_1\, z_2>$ [22] and in a disentangled state with density operator

$$\rho(0) = \rho_a(0) \otimes \rho_b(0) = |\psi(0)><\psi(0)|, \tag{8}$$

where $\rho_a(0)$ and $\rho_b(0)$ are density operators at $t = 0$ of the field modes, and

$$|\psi(0)> = \sum_{m_1=0}^{\infty}\sum_{m_2=0}^{\infty} C_{m_1 m_2}(0)|m_1> \otimes |m_2>, \tag{9}$$

with expansion coefficients $C_{n_1n_2}(0) \equiv < n_1n_2|z_1z_2 >$ [8,9]. Thus, we write

$$C_{m_1m_2}(0) = [\rho_{m_1m_1}(0)\rho_{m_2m_2}(0)]^{1/2}, \tag{10}$$

where $\rho_{m_jm_j}(0)$ ($j = 1, 2$) are the diagonal density matrix elements in the initial state. Note that it is not necessary to assume that at $t = 0$ the two modes have the same photon distribution, i.e., the time evolution of the field density operator is written quite generally as

$$\rho(t) = \sum_{n_1=0}^{\infty}\sum_{n_2=0}^{\infty}\sum_{m_1=0}^{\infty}\sum_{m_2=0}^{\infty} C_{n_1}(t)C_{n_2}(t)C^*_{m_1}(t)C^*_{m_2}(t)\mathcal{P}^{n_1m_1}_{n_2m_2}, \tag{11}$$

where $\mathcal{P}^{m_1n_1}_{m_2n_2} = |m_1n_1 > \otimes < m_2n_2|$ is the two-mode Fock space projection operator. The time dependent coefficients in Eq. (11) can be written as

$$C_{n_1n_2}(t) = C_{n_1n_2}(0)\Xi_{n_1n_2}(t), \tag{12}$$

where $\Xi_{n_1n_2}(t)$ are the complex eigenvalues of the evolution operator, i.e.,

$$\Xi_{n_1n_2}(t) = \exp\left[-it\,\frac{g^2}{\Delta}(4\,n_1\,n_2\,-\,n_1^2)\right]. \tag{13}$$

2.2. Boson squeezing and homomorphism with the unitary group

The initially coherent cavity field can be squeezed when it interacts either with a single atom or with a group of N two-level atoms, which is placed in a volume with dimensions small compared to the wavelength associated with the atom's two-level dipole and evolves on time scales shorter than any $\mathcal{J}^2$-breaking relaxation mechanism, an example of which is an angular momentum system, which has collective atomic raising and lowering operators, $\mathcal{J}_+$ and $\mathcal{J}_-$, with a fixed spin quantum number $\mathcal{J} = N/2$ [8].

Let us introduce the Hermitian operator involving the a mode as follows

$$X_\theta = 1/2(a^k e^{-i\theta} + a^{\dagger k}e^{i\theta}) \quad (k = 1 \quad \text{or} \quad 2), \tag{14}$$

which for $\theta = 0$ corresponds to the in-phase quadrature component of the field and for $\theta = \pi/2$ to the out-of-phase component. Quantum fluctuations of the quadrature components of the field are measured by their variances. Thus, squeezing is said to exist whenever the uncertainty of one of the quadratures is below the vacuum level (standard quantum limit). In terms of the variances

$$\langle(\Delta X_\theta)^2\rangle = \langle X_\theta^2\rangle - \langle X_\theta\rangle^2 = \frac{1}{2}(\cos 2\theta Re\langle a^{2k}\rangle + \sin 2\theta Im\langle a^{2k}\rangle$$
$$+ \delta_{k2}\langle a^{\dagger 2}a^2\rangle + k\langle a^\dagger a\rangle + k/2) - (\cos\theta Re\langle a^k\rangle + \sin\theta Im\langle a^k\rangle)^2, \tag{15}$$

the based Heisenberg uncertainty relation conditions for squeezing are

$$0 < V(\tau) \equiv 1 - 4\langle(\Delta X_\theta)^2\rangle \le 1, \tag{16}$$

for $k = 1$ (Hong and Mandel approach [17,18]) and

$$Z(\tau) \equiv \langle(\Delta X_\theta)^2\rangle/(\bar{n}_1 + 1/2) < 1, \tag{17}$$

for $k = 2$ (Hillery approach [16]). This latter condition corresponds to the amplitude squared (higher-order) squeezing.

The squeezing phenomenon of the present nonlinear optical process can be further explored by considering conventional interferometers which are devices characterized, in general, by $SU(2)$. To this end we introduce the Schwinger realization of the $SU(2)$ generators of the angular momentum operators associated to the field modes

$$\mathcal{J}_x = \frac{1}{2}(a^\dagger b + b^\dagger a); \quad \mathcal{J}_y = -\frac{i}{2}(a^\dagger b - b^\dagger a); \quad \mathcal{J}_z = \frac{1}{2}(a^\dagger a - b^\dagger b), \tag{18}$$

and the number operator

$$\mathcal{N} = a^\dagger a + b^\dagger b. \tag{19}$$

The operators in Eq. (18) satisfy the commutation relations for the Lie algebra of $SU(2)$ and the Casimir invariant for this group, using Eqs. (18) and (19), can be put into the form

$$\mathcal{J}^2 = \frac{\mathcal{N}}{2}\left[\frac{\mathcal{N}}{2} + 1\right]. \tag{20}$$

In fact, $\mathcal{N}$ itself commutes with all the operators of Eq. (18).

We now characterize a lossless passive device with two input ports and two output ports with the operators of Eqs. (18) and (19) and consider a beam splitter with the scattering matrix [23]

$$\mathcal{S} = \begin{pmatrix} e^{i\gamma_1} & 0 \\ 0 & e^{i\gamma_2} \end{pmatrix}. \tag{21}$$

This scattering matrix induces a transformation of $\mathcal{J}$ according to

$$\mathcal{S} \to \begin{pmatrix} \mathcal{J}_\chi \\ \mathcal{J}_\xi \\ \mathcal{J}_\zeta \end{pmatrix} = e^{i\delta\mathcal{J}_z}\begin{pmatrix} \mathcal{J}_x \\ \mathcal{J}_y \\ \mathcal{J}_z \end{pmatrix} e^{-i\delta\mathcal{J}_z}, \tag{22}$$

which represents an homomorphism with the unitary group, i.e., a rotation about the z axis by the angle $\delta = \gamma_2 - \gamma_1$ corresponding to the relative phase shift between the two light beams. In fact, since $SU(2)$ is equivalent to the rotation group in three dimensions, this homomorphism allows one to visualize the operations of beam splitters and phase shifters as rotations in 3-space.

Angular momentum systems have often been regarded as squeezed if the uncertainty of one component, say $< \Delta\mathcal{J}_x^2 >$ or $< \Delta\mathcal{J}_y^2 >$, is smaller than $1/2|< \mathcal{J}_z >|$ or equivalently, if $< \Delta\mathcal{J}_\chi^2 >$ or $< \Delta\mathcal{J}_\xi^2 >$, is smaller than $1/2|< \mathcal{J}_\zeta >|$, where invariance of the commutation relations under rotations in Eq. (22) is used. It was claimed that this definition implies that a coherent spin state is already squeezed if it is placed in an appropriate system of coordinates, and also that angular momentum can be squeezed by just rotating the coherent angular momentum state [24]. In spin systems for example, the squeezing occurs on the phase sphere (spherical phase space). Unlike boson squeezing, the quasiprobability distribution cannot be homogeneously or globally squeezed in one direction over the whole phase space. If a spin component is shrunk around a certain point on the sphere, it must be stretched around another point. This imposes a fundamental restriction on the reduction in quantum noise [24].

The connection between a linear lossless passive device having two input ports and two output ports and the group $SU(2)$ will be exploited, through numerical simulations, to explore the squeezing phenomenon in these angular momentum operators. Thus, fluctuations in the component $\mathcal{J}_\alpha$ ($\alpha = \chi, \xi$ or x, y) are said to be squeezed if $\mathcal{J}_\alpha$ satisfies the based Heisenberg uncertainty relation condition

$$Y(\mathcal{J}_\alpha) = \Delta\mathcal{J}_\alpha - \left(\frac{|\langle\mathcal{J}_\zeta\rangle|}{2}\right)^{1/2} < 0, \tag{23}$$

with the variance $\Delta\mathcal{J}_\alpha = [\langle\mathcal{J}_\alpha^2\rangle - \langle\mathcal{J}_\alpha\rangle^2]^{1/2}$.

2.3. Entanglement and higher-order entanglement

There exist several inseparability criteria [3,25] that are expressed in terms of expectation values of field operators and thus suitable for study of entanglement dynamics within the framework of the present approach. Among these criteria, the Hillery–Zubairy criteria I and II (HZ-I and HZ-II) [26–28] have received more attention for various reasons, such as computational simplicity, experimental realizability, and their recent success in detecting

entanglement in various optical, atomic, and optomechanical systems [11,29]. Specifically, Hillery and Zubairy introduced two criteria for intermodal higher-order entanglement [26] as follows:

$$E_{ab}^{m,n} = \langle a^{\dagger m} a^m b^{\dagger n} b^n \rangle - |\langle a^m b^{\dagger n} \rangle|^2 < 0, \tag{24}$$

and

$$E'^{m,n}_{ab} = \langle a^{\dagger m} a^m \rangle \langle b^{\dagger n} b^n \rangle - |\langle a^m b^n \rangle|^2 < 0. \tag{25}$$

Here m and n are nonzero positive integers and the lowest possible values of m and n are $m = n = 1$. A quantum state will be referred to as a (bipartite) higher-order entangled state if it is found to satisfy Eq. (24) and/or Eq. (25) for any choice of integer m and n satisfying $m + n \geq 3$ [3].

The required matrix elements involved in Eq. (24) are given by

$$\langle a^{\dagger m} a^m b^{\dagger n} b^n \rangle = \sum_{n_1=0}^{\infty} \sum_{n_2=0}^{\infty} \rho_{n_1 n_1}(0) \rho_{n_2 n_2}(0) \frac{n_1! n_2!}{(n_1 - m)!(n_2 - n)!}, \tag{26}$$

and

$$|\langle a^m b^{\dagger n} \rangle|^2 = \left| \sum_{n_1=0}^{\infty} \sum_{n_2=0}^{\infty} \left[\rho_{n_1 - m\, n_1 - m}(0) \rho_{n_2 + n\, n_2 + n}(0) \rho_{n_1 n_1}(0) \rho_{n_2 n_2}(0) \right]^{1/2} \left[\frac{n_1!(n_2 + n)!}{n_2!(n_1 - m)!} \right]^{1/2} \exp\left(i\tau P_{n_1 n_2}(m, n) \right) \right|^2, \tag{27}$$

where $P_{n_1 n_2}(m, n) = 4(n_1 n - m n_2 - m n) + m(2 n_1 - m)$, while those required in Eq. (25) are computed as

$$\langle a^{\dagger m} a^m \rangle = \sum_{n_1=0}^{\infty} \sum_{n_2=0}^{\infty} \rho_{n_1 n_1}(0)\, \rho_{n_2 n_2}(0) \left[\frac{n_1!}{(n_1 - m)!} \right], \tag{28}$$

$$\langle b^{\dagger n} b^n \rangle = \sum_{n_1=0}^{\infty} \sum_{n_2=0}^{\infty} \rho_{n_1 n_1}(0)\, \rho_{n_2 n_2}(0) \left[\frac{n_2!}{(n_2 - n)!} \right], \tag{29}$$

and

$$|\langle a^m b^n \rangle|^2 = \left| \sum_{n_1=0}^{\infty} \sum_{n_2=0}^{\infty} \left[\rho_{n_1 - m\, n_1 - m}(0) \rho_{n_2 - n\, n_2 - n}(0) \rho_{n_1 n_1}(0) \rho_{n_2 n_2}(0) \right]^{1/2} \left[\frac{n_1! n_2!}{(n_1 - m)!\,(n_2 - n)!} \right]^{1/2} \exp\left(i\tau Q_{n_1 n_2}(m, n) \right) \right|^2, \tag{30}$$

where $Q_{n_1 n_2}(m,\ n) = 4(m n - m n_2 - n_1 n) + m(2 n_1 - m)$.

It is interesting to investigate the dynamics of entanglement from the information theory point of view. To achieve this goal we use a particular entanglement measure, namely, the linear entropy which does not require diagonalization of the density matrix and is a measure of mixedness in quantum states. It is a scalar defined as

$$S_L(\tau) = -Tr\, \rho(\tau) lg_2 \rho(\tau) \simeq \frac{1}{\ln 2} \left[1 - Tr\, \rho_a^2(\tau) \right]$$
$$= \frac{1}{\ln 2} (1 - Tr\ \ [Tr_b\, \rho(\tau)]^2). \tag{31}$$

It is noted that the expression of $S_L(t)$ is representation-independent since the trace is invariant under unitary transformations of the model. In the language of entanglement and omitting the $1/\ln 2$ factor in Eq. (31), $S_L(\tau)$ ranges from 0 (i.e., $Tr\rho^2(\tau) = 1$) for a disentangled and/or pure states to 1 (i.e., $Tr\rho^2(\tau) = 0$) for maximally entangled bipartite. Thus, $Tr\rho^2(\tau)$ can be taken as the Bloch sphere radius.

It is well known that the quantum coherences which are built up during the interaction process significantly affect the dynamics of the field. Thus, in order to investigate the nonclassical behavior of the present model we discuss in the next section the results derived from the numerical computation of these nonclassical effects.

3. Numerical simulations and coherent states

Conventional coherent states constitute a family of collective states of the harmonic oscillator parametrized by a single complex number. These coherent states are an extremely efficient and flexible tool to treat very different aspects of quantum problems. The actual key for utility of coherent states is their property associated to the resolution of unity, or completeness, which allows one to use them as a (usually non-orthogonal) basis. The computations of the nonclassical squeezing and quantum entanglement effects were conducted separately in terms of the dimensionless parameter $\tau = tg^2/\Delta$ using four different initial coherent states for the initial state, given in Eqs. (32)–(35). In these coherent states z_j is a complex number and $|z_j|^2$ is generally associated with the mean photon number of mode j; $\mathcal{N}_{\alpha,\beta}(|z_j|^2)$, $\mathcal{N}_{\kappa}(|z_j|^2)$, and $\mathcal{N}_{M}(|z_j|^2)$ are normalization factors.

Fig. 1 shows the evolution of the based Heisenberg uncertainty relation variance for normal squeezing factor and amplitude squared squeezing of the field in the quadrature a mode computed from Eq. (16) (panel) and Eq. (17) (lower panel) respectively. In this figure it was assumed that the field modes are initially prepared in the Mittag-Leffler coherent state (α, $\beta > 0$) [30]

$$|z_j; \alpha, \beta> = \left[\mathcal{N}_{\alpha,\beta}\left(|z_j|^2 \right) \right]^{-1/2} \sum_{n_j=0}^{\infty} \frac{z_j^{n_j}}{\sqrt{\Gamma(\alpha n_j + \beta)}} |n_j>, \tag{32}$$

It is observed a small fractional squeezing (about 15%) in the normal squeezing factor (upper panel) with the amplitudes regularly spaced ($\Delta\tau \sim 1.57$). Clearly it is not observed any signature of squeezing in a mode during these rather large intervals of τ, out of the envelopes. Actually, this particular squeezing phenomenon corresponds to Poisson distributions, peaked at $\tau = 1.57r$ ($r = 1, 2, \ldots$). Amplitude squared squeezing in this quadrature variable, on the other hand, is always present, as lower panel shows. Here the Poisson distributions are *inverted*, peaked at $\tau = 0.72r$ at these intervals, and the amount of continuous squeezing is close to 99.9%.

Fig. 2 shows the variation of the variance squeezing factor $V(\mathcal{J}_\alpha)$ ($\alpha = \chi, \xi$) based on the Heisenberg uncertainty relation of angular momentum rotated components computed from Eq. (23). The field modes are initially prepared in the two-parameter set of states ($\kappa > -1$) [31] for both modes (upper panel)

$$|z_j; \kappa> = \left[\mathcal{N}_{\kappa}\left(|z_j|^2 \right) \right]^{-1/2} \sum_{n_j=0}^{\infty} \left[\frac{\Gamma(n_j + \kappa + 1)}{n_j!\Gamma(\kappa + 1)} \right]^{1/2} \left(\frac{z_j}{\sqrt{\kappa + 1}} \right)^{n_j} |n_j>, \tag{33}$$

while Poisson photon distribution

$$|z_j> = \exp(-|z_j|^2/2) \sum_{n_j=0}^{\infty} \frac{z_j^{n_j}}{\sqrt{n_j!}} |n_j>, \tag{34}$$

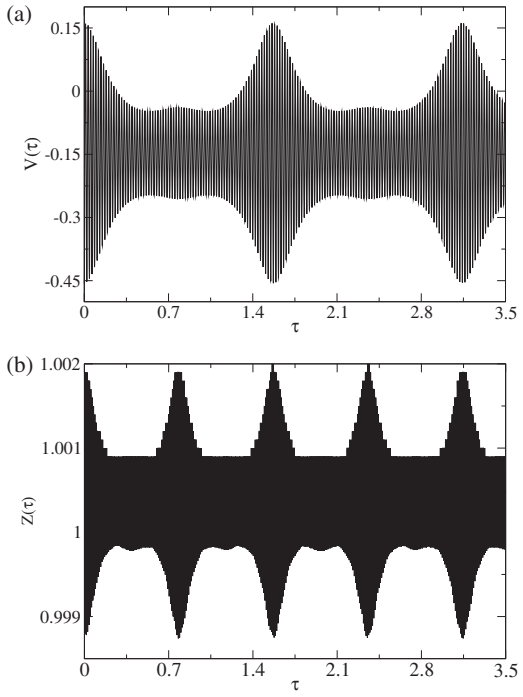

Fig. 1. (a) Upper panel: based Heisenberg uncertainty relation variance squeezing factor of the boson operators for mode a, $a(a^{\dagger})$. The field is initially prepared in the Mittag-Leffler coherent state of Eq. (32) for modes a and b, with $\alpha = 0.23$; $\beta = 1.4$; $\bar{n}_1 = 4$; $\bar{n}_2 = 15$; $\theta = 0$; $k = 1$ (Eq. (16)). (b) Lower panel: same as (a) but $k = 2$. This corresponds to the amplitude squared squeezing factor (Eq. (17)).

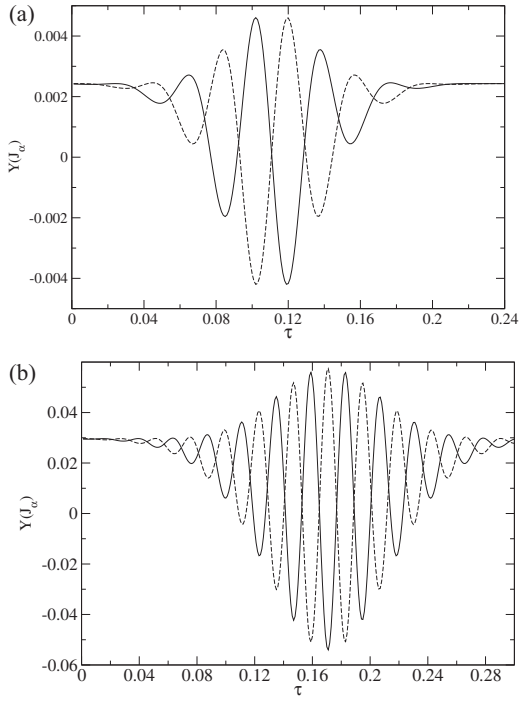

Fig. 2. (a) Upper panel: based Heisenberg uncertainty relation variance squeezing factor $Y(J_\alpha)$ (Eq. (23)). This field is initially prepared in the two parameter set of coherent states of Eq. (33) for modes a and b, with $\kappa = 48$; $\bar{n}_1 = 0.001$; $\bar{n}_2 = 15$; $\delta = \pi/4$. Solid line: $Y(J_\chi)$; dashed line: $Y(J_\xi)$. (b) Lower panel: same as (a) but with the field initially prepared in the Poisson coherent state of Eq. (34) for mode a and in the binomial coherent state of Eq. (35) for mode b, with $M = 79$; $\bar{n}_1 = 0.001$; $\bar{n}_2 = 25$; $\delta = \pi/2$.

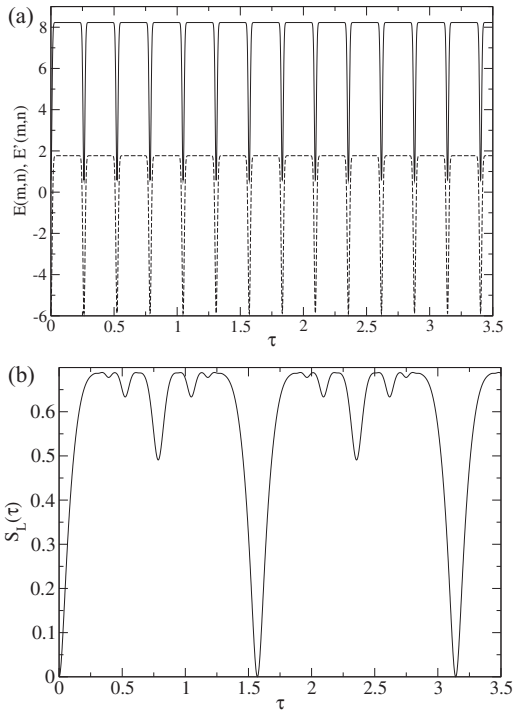

Fig. 3. (a) Upper panel: higher-order quantum entanglement computed using the Hillery–Zubairy criteria. $m = 6$; $n = 3$; $\bar{n}_1 = 4$; $\bar{n}_2 = 15$. Solid line: entanglement computed from Eq. (24) (HZ-I); dashed line: entanglement computed from Eq. (25) (HZ-II). The field is initially prepared in the Poisson coherent state for mode a and in the binomial coherent state for mode b, with $M = 80$. (b) Lower panel: information entropy computed from Eq. (36) with $\bar{n}_1 = 4$ and $\bar{n}_2 = 1$, and the field modes are initially prepared in the Poisson coherent state. The $\ln 2$ factor in Eq. (31)) was omitted in this calculation.

and binomial boson coherent states [32]

$$|z_j; M> = \left[\mathcal{N}_M\left(|z_j|^2\right)\right]^{-1/2} \sum_{n_j=0}^{M} \frac{M!}{(M-n_j)!\sqrt{n_j!}} z_j^{M-n_j} |n_j>, \qquad (35)$$

were used for modes a and b respectively (lower panel). It can be observed that the second-order variance predicts no squeezing in both components of $\mathcal{J}_\alpha$ for $\tau < 0.06$ and $\tau > 0.16$ (upper panel) and for $\tau < 0.08$ and $\tau > 0.22$ (lower panel). The squeezing only appears during short periods of τ, keeping the magnitude of the fluctuations above and below of zero with a nearly constant period. The overall behavior in both panels shows that both components are alternatively squeezed and unsqueezed, thus preserving the uncertainty relation.

Fig. 3a (left panel) shows the higher-order intermodal quantum entanglement between modes a and b, with $m = 6$ and $n = 3$, plotted with rescaled interaction of $E(m, n)$ and $E'(m, n)$ in Eqs. (24) and (25). The field modes are initially prepared in the Poisson (Eq. (34)) and binomial coherent states (Eq. (35)) for modes a and b respectively. It is observed that HZ-I criterion computed from Eq. (24) (solid line) fails to detect any entanglement in the present case. However, it does not indicate that the modes are separable as both the HZ-I and HZ-II inseparability criteria are only necessary and not essential. On the other hand, the existence of entanglement is clearly detected by HZ-II criterion computed from Eq. (25) (dashed line) in this particular case. Here the entangled process shows a series of minima at regular intervals of $\Delta\tau = 0.26$.

We now turn to the linear entropy as a criterion of entanglement. Assuming a Poisson distribution in the initial state $\tau = 0$, performing a partial trace over the second harmonic mode, squaring the resultant expression, and then taking the trace over the

fundamental mode in Eq. (31), one arrives to the following compact form for the linear entropy

$$S_L(\tau) = 1 - e^{-2\bar{n}_1} \sum_{n_1=0}^{\infty} \sum_{m_1=0}^{\infty} \exp\left[-4\,\bar{n}_2 \sin^2[2\,\tau\,(n_1 - m_1)]\right] \frac{|\bar{n}_1^{(n_1+m_1)}}{n_1!\,m_1!}. \tag{36}$$

The unitary evolution of the linear entropy is plotted in Fig. 3b (lower panel), where it was assumed a Poisson distribution for the secondary mode. It can be observed that at the initial state $\tau = 0$ the model becomes completely disentangled, according to the hypothesis of Eq. (8). After a very short initial τ the entanglement has a rapid rise and the entropy saturates to a relatively stable value with continuous oscillations of small amplitudes, with the magnitude of the entropy keeping below of 70% of the optimum value. The maximum entanglement $S_{L\,max}$ here can be considered as entangling powers of unitary operations, describing the capability of entropy production. The present nonlinear process shows that, from the information theory point of view, the dynamics of entanglement is a periodic function, with a period of $p_r = 2\,\tau_r$, where τ_r is the localization of the principal minima, i.e., $\tau_r = r\,\pi/4(n_1 - m_1)$. Near the periods there is a strong decrease of the linear entropy and the system returns to an almost disentanglement state.

4. Final remarks

The nonclassical higher-order squeezing and quantum entanglement effects were investigated in the SHG using different initial coherent states (generalized squeezed states) for the two-mode Hamiltonian. It was observed that the based Heisenberg uncertainty relation variance of the fundamental mode shows a small fractional but continuous magnitude of the normal squeezing factor, while amplitude squared squeezing in this quadrature variable is always present. The introduction of a simple scattering matrix induces a transformation of the angular momentum components through an homomorphism with the unitary group, which allows one to visualize the operations of beam splitters and phase shifters as rotations in 3-space. Thus, the variance squeezing factors based on the Heisenberg uncertainty relation of these angular momentum components show that the rotated components are alternatively squeezed and unsqueezed, thus preserving the uncertainty relation. These states with the reduced quantum noise in one of the quadrature components are in fact, very important for the problems of measurement of weak forces and signals, in particular, for the detectors of gravitational waves and interferometers.

Two criteria of higher-order intermodal quantum entanglement were used. It was found that the HZ-I criterion fails to detect any entanglement, while the existence of this nonclassical effect was clearly detected by HZ-II criterion.

The use of a particular entanglement measure for the present nonlinear optical model shows that the dynamics of entanglement is a periodic function and that the modulus of the Bloch vector is not preserved during the time evolution of the linear entropy. The maximum entanglement occurs within small intervals of τ, where the linear entropy represents steady states that are clearly mixed states and the study of quantum entanglement for mixed states is a very active field of inquiry. It immediately raises the question of whether the entanglement can be distilled and used as a resource for some quantum communication or computation task. In particular, the use of different initial coherent states for the first and second mode is a crucial feature of the present nonlinear optical model, since one can adjust one mode while monitoring the other in order to optimize the signal/noise relation.

Acknowledgments

This project is supported by research grants in aid from the University of Buenos Aires (Project No. 20020130100226BA), and the Consejo Nacional de Investigaciones Científicas y Técnicas (CONICET, PIP No. 112 201301 00377CO, Res. D No 5013/14, República Argentina). The author is grateful to the Department of Physics and IFIBA, Facultad de Ciencias Exactas y Naturales, University of Buenos Aires, for facilities provided during the course of this work.

References

[1] M. Han, G. Giese, J. Bille, Second harmonic generation imaging of collagen fibrils in cornea and sclera, Opt. Express 13 (2005) 5791–5797.
[2] D.J. Brown, N. Morishige, A. Neekhra, D.S. Minckler, J.V. Jester, Application of second harmonic imaging microscopy to assess structural changes in optic nerve head structure *ex vivo*, J. Biomed. Opt. 12 (2007) 024029 (5 pages).
[3] K. Thapliyal, A. Pathak, B. Sen, J. Peřina, Higher-order nonclassicalities in a codirectional nonlinear optical coupler: quantum entanglement, squeezing, and antibunching, Phys. Rev. A 90 (2014) 013808 (8 pages and references therein).
[4] M. Hillery, Quantum cryptography with squeezed states, Phys. Rev. A 61 (2000) 022309 (8 pages).
[5] A. Furusawa, J.L. Sorensen, S.L. Braunstein, C.A. Fuchs, H.J. Kimble, E.S. Polzik, Unconditional quantum teleportation, Science 282 (1998) 706–709.
[6] A.K. Ekert, Quantum cryptography based on Bell's theorem, Phys. Rev. Lett. 67 (1991) 661–663.
[7] C.H. Bennett, G. Brassard, C. Crepeau, R. Jozsa, A. Peres, W.K. Wootters, Teleporting an unknown quantum state via dual classical and Einstein–Podolsky–Rosen channels, Phys. Rev. Lett. 70 (1993) 1895–1899.
[8] H. Grinberg, Nonclassical effects in a highly nonlinear generalized homogeneous Dicke model, Ann. Phys. 326 (2011) 2845–2867.
[9] H. Grinberg, Variance squeezing and information entropy squeezing via Bloch coherent states in two-level nonlinear spin models, Optik 125 (2014) 5566–5572.
[10] A. Pathak, J. Křepelka, J. Peřina, Relation between squeezing of vacuum fluctuations, quantum entanglement and sub-shot noise in Raman scattering, Phys. Lett. A 377 (2013) 2692–2701.
[11] B. Sen, S.K. Giri, S. Mandal, C.H. Raymond Ooi, A. Pathak, Intermodal entanglement in Raman processes, Phys. Rev. A 87 (2013) 022325 (9 pages).
[12] A. Verma, A. Pathak, Higher order squeezing and higher order subPoissonian photon statistics in intermediate states, Phys. Lett. A 374 (2010) 1009–1020.
[13] A. Allevi, S. Olivares, M. Bondani, Measuring high-order photon-number correlation in experiments with multimode pulsed quantum states, Phys. Rev. A 85 (2012) 063835 (5 pages).
[14] A. Allevi, S. Olivares, M. Bondani, High-order photon-number correlations: a resource for characterization and applications of quantum states, Int. J. Quantum Inf. 10 (2012) 1241003 (8 pages).
[15] M. Avenhaus, K. Laiho, M.V. Chekhova, C. Silberhorn, Accessing higher order correlations in quantum optical states by time multiplexing, Phys. Rev. Lett. 104 (2010) 063602 (4 pages).
[16] M. Hillery, Amplitude-squared squeezing of the electromagnetic field, Phys. Rev. A 36 (1987) 3796–3802.
[17] C.K. Hong, L. Mandel, Higher-order squeezing of a quantum field, Phys. Rev. Lett. 54 (1985) 323–325.
[18] C.K. Hong, L. Mandel, Generation of higher-order squeezing of quantum electromagnetic fields, Phys. Rev. A 32 (1985) 974–982.
[19] A.B. Klimov, S.M. Chumakov, A Group-Theoretical Approach to Quantum Optics, Wiley-VCH Verlag GmbH & Co. KGaA, Weinheim, 2008, pp. 77–78 (304–306).
[20] A.B. Klimov, L.L. Sánchez-Soto, Method of small rotations and effective Hamiltonians in nonlinear quantum optics, Phys. Rev. A 61 (2000) 063802 (11 pages).
[21] A.B. Klimov, L.L. Sánchez-Soto, A. Navarro, E.C. Yustas, Effective Hamiltonians in quantum optics: a systematic approach, J. Mod. Opt. 49 (2002) 2211–2226.
[22] R.J. Glauber, Coherent and incoherent states of the radiation field, Phys. Rev. 131 (1963) 2766–2788.
[23] B. Yurke, S.L. McCall, J.R. Klauder, *SU*(2) and *SU*(1, 1) interferometers, Phys. Rev. A 33 (1986) 4033–4054.
[24] M. Kitagawa, M. Ueda, Squeezed spin states, Phys. Rev. A 47 (1993) 5138–5143.
[25] G.S. Agarwal, A. Biswas, Inseparability inequalities for higher order moments for bipartite systems, New J. Phys. 7 (2005) 211 (7 pages).
[26] M. Hillery, M.S. Zubairy, Entanglement conditions for two-mode states, Phys. Rev. Lett. 96 (2006) 050503 (4 pages).
[27] M. Hillery, M.S. Zubairy, Entanglement conditions for two-mode states: applications, Phys. Rev. A 74 (2006) 032333 (7 pages).
[28] M. Hillery, H.T. Dung, H. Zheng, Conditions for entanglement in multipartite systems, Phys. Rev. A 81 (2010) 062322 (6 pages).

[29] S.K. Giri, B. Sen, C.H. Raymond Ooi, A. Pathak, Single-mode and intermodal higher-order nonclassicalities in two-mode Bose–Einstein condensates, Phys. Rev. A 89 (2014) 033628 (10 pages).
[30] J.-M. Sixdeniers, K.A. Penson, A.I. Solomon, Mittag–Leffler coherent states, J. Phys. A: Math. Gen. 32 (1999) 7543–7563.
[31] Y. Aharonov, H.W. Wang, J.M. Knight, E.C. Lerner, Generalized distribution operators and a new method in group theory, Lett. Nuovo Cimento 2 (1971) 1317–1322.
[32] J.-M. Sixdeniers, K.A. Penson, On the completeness of coherent states generated by binomial distribution, J. Phys. A: Math. Gen. 33 (2000) 2907–2916.